June 1988 LRP 350/88

AN IMPROVED BARIUM PLASMA SOURCE FOR Q-MACHINES

P.J. Paris, N. Rynn, S. Roe, P. Gorgerat
A. Simik, M. Schleipen

AN IMPROVED BARIUM PLASMA SOURCE FOR Q-MACHINES

P.J. Paris, N. Rynn*, S.Roe*, P. Gorgerat, A. Simik, M. Schleipen**

Centre de Recherches en Physique des Plasmas

Association Euratom - Confédération Suisse

Ecole Polytechnique Fédérale de Lausanne

21, Av. des Bains, CH-1007 Lausanne / Switzerland

* University of California at Irvine, Irvine, California, U.S.A.

** ASEA - Brown Boveri and Co, Oerlikon, Switzerland

INTRODUCTION

We report on the development of a barium plasma source which uses a three-stage gun stabilized in temperature by means of a computerized power supply. This stabilization allows the rhenium-plated tungsten hot plate to operate at a constant temperature for many hours.

The assembly for vaporizing barium is heated by coaxial resistive wires which are fed by current controlled power supplies. The homogeneity of the barium illumination of the hot plate is provided by an annular effuser with a 360° aperture slit.

The plasma radial density profiles are symmetrical and flat over 3.5 cm diameter. Density flatness is within 3% to 5% in that radial dimension and local temporal $\delta n/n$ is less than .3%.

Plasma production characteristics such as these are highly desirable in basic plasma research, where spatial and temporal unformity are prerequisites to successful investigations.

I. ALKALI PLASMA PRODUCTION [1,2]

A Q-machine plasma is produced by spraying an alkali or alkaline earth metallic vapor on a hot plate surface such as tantalum, tungsten or rhenium. In order to get an homogeneous plasma, a uniformly heated plate, with the appropriate work function, is needed. The

temperature of the hot plate is of the order of 2100°K to 2500°K. The plasma is produced by contact ionization : the atomic metal vapor, typically of potassium, cesium, or barium atoms, is directed from an effuser onto the refractory metal hot plate. The metallic vapor comes into thermodynamic equilibrium with the hot plate surface and is ionized with an efficiency given by the Langmuir-Saha equation :

$$n_i/n_0 = g_i/g_0 \exp\left(e(\phi_w-\phi_i)/kT\right) \qquad (1)$$

where n_i is ion density, n_0 is neutral density, g_i/g_0 is the ratio of statistical weights of the ionic to neutral states and is $\approx 1/2$ for alkali metal atoms, ϕ_w is the work function of the hot plate, ϕ_i isionization potential, and kT is the temperature of hot plate in eV.

In order to obtain optimal ionization efficiency, one must choose a combination of hot plate material and species of atomic vapor which yields the smallest difference in work function and ionization potential, respectively. In the typical operating case of rhenium (ϕ_w=4.74 to 5.1eV) plated tungsten hot disc at 2200°K and with barium vapor (ϕ_i=5.21eV), the ionization efficiency is between 16% and 50%, depending upon the value of ϕ_w for rhenium. Nevertheless, the plasma in the test chamber is almost fully ionized because the neutral atoms are condensed on the cooled vacuum chamber walls.

In the ionization process, a valence electron of an atom in the metallic vapor is captured in the metal surface of the hot plate, while the plate emits electrons thermionically to maintain charge neutrality in the main body of plasma. A plasma sheath exists at the hot plate; the character of this sheath is determined by the balance

of electron and ion currents at the hot plate. We typically produce plasmas which are in the electron rich regime, that is to say that the electron density at the hot plate produced by thermionic emission exceeds the ion density produced by contact ionization on the hot plate. The critical density is given by :

$$n_c = 4A_R T^2/eV_e \cdot \exp(-e\phi_w/kT) \qquad (2)$$

where A_R is the Richardson constant, eV_e is the average energy of the electrons.

This equation delimits electron rich and ion rich operating regimes. For the parameters given above, the critical density is approximatelly 3 x $10^9 cm^{-3}$, and we operate below this value, in the electron rich regime.

II. THE PLASMA GUN

A. Hot plate subsystem

The high temperature source consists of three stages : a filament ribbon, a lanthanum hexaboride cathode and a rhenium-plated tungsten plate (Fig. 1). The hot plate gun is described in Ref. 3 and has been improved in recent years. When starting the gun, the second two stages are heated by electron bombardment from the first two stages. In order to collimate the electron beams, the gun is operated in an axial magnetic field aligned parallel to the gun. In steady state operation,

a stable equilibrium is achieved with electron bombardment of the hot plate and thermal radiation by the plate onto the cathode.

The filament is composed of a tungsten ribbon and of a tantalum ribbon in order to provide both mechanical strength and good electron emission. In order to decrease the effect of the $\underline{j} \times \underline{B}$ force on the filament, the magnetic field is kept at a low value (.02 Tesla) while the filament is on. This procedure increases the life of the filament.

The cathode is made of a multi-grooved molybdenum disc filled with lanthanum hexaboride (LaB_6) powder. After being dissolved in anhydrous amyle acetate, the LaB_6 powder is pressed into the grooves. LaB_6 has been chosen because of its low work function (ϕ_W=2.66eV), and thus it yields an adequate electron emission at these operating temperatures. Furthermore, LaB_6 exhibits a certain impervious nature to oxide contamination which allows occasional exposures to dry atmosphere. In order to obtain homogeneous electron emission, the thickness of the molybdenum disc was taken to be 6 mm. Four molybdenum rods hold the cathode rigidly to prevent any motion during operation. These rods are small enough to produce only a minor heat loss.

The hot plate is a tungsten disc of 6.25 mm thickness and 5 cm diameter. To increase the work function at the ionizing surface, a rheninum plating is deposited electrolytically (4). The rhenium work function (4.74 to 5.1 eV) is the closest known choice to the ionization potential of barium (5.21 eV). The hot plate is electron beam welded to a tantalum tube of .5 mm thickness which is rigid, but not a large heat loss. The tube also provides confinement of the cathode heat. Alignment is achieved by use of a molybdenum cylinder

(barillet) and two glass-ceramic insulating barillets. Ceramic alumina tubes fit around the molybdenum rods for high voltage insulation.

The filament-cathode assembly is introduced in a stainless steel tube with side-slots and holes to enable rapid pumping of any outgassing. One should note that because of the use of high voltage, outgassing may produce arcing. Considerable efforts have been made in order to reduce this phenomenon.

The hot plate is connected to the stainless steel tube holder flange via three boron nitride spacers.

A bench positionning set up jig simplifies the task of alignment. It also helps in centering the 360° slotted effuser from which the barium is sprayed over the hot plate. In order to produce a flat radial density profile the effuser is positioned axially at a particular distance from the hot plate. To improve temperature and therefore density uniformity, a ring heat shield of tantalum covers the extremity of the hot plate; this reduces radiative loss and keeps the tungsten disc edge temperature at a high value.

In order to prevent bombardment of the molybdenum barillet or the glass-ceramic elements by fast electrons from the filament, a tantalum screen is placed on the filament holder.

Heat radiation from the hot plate keeps the LaB_6 cathode at working temperature but it also can produce undesirable outgassing from the glass-ceramic pieces. Two tantalum screens are placed to reduce this effect.

B. The barium vaporizing subsystem

The plasma gun is realized by adding to the hot plate subsystem a barium vaporizing assembly. This assembly consists of two main parts : the barium oven and the heated pipe which connects to the effuser (Fig. 2). Barium metal requires a relatively high temperature to melt (725°C). A stainless steel oven, surrounded by an electrical heater wire, is connected to the effuser through a heated pipe. The top cover of the oven can also be heated in order to prevent solidification of the condensed vapor on the cover when power is turned down. This optimizes the vaporization of Ba contained in the oven. In order to keep the oven interface hermetically tight even at high temperature the seal is made "knife shaped". The tube connecting to the effuser is made in the same fashion but brought through a "bayonet" lock. Heat shields surrounding the oven and the tube enhance heating efficiency.

The effuser has an inner baffle design which allows barium vapor to leak through the thin 360° slot uniformly. Although the oven and intermediate tube are resistively heated, the effuser only receives heat radiation from the hot plate. Two stainless steel heat shields are used to present radiative heat loss from the effuser.

C. Integration of the plasma gun in a water cooled jacket

The whole gun is placed inside a water cooled jacket heat shield (Fig. 3). This enables mechanical centering of the gun in the vacuum vessel within .5 mm accuracy. The barium neutral flux, which is not ionized, is largely condensed on the cooled jacket. This reduces the

deposition of barium on the rest of the device. Therefore, probes and optical elements which are not in the plasma, remain free of barium for a longer period.

Additional baffles are placed in front of the jacket aperture in order to reduce heat radiation from the hot plate as well as straylight. This also avoids heating of the diagnostic trolleys which are described elsewhere.[4] Four thermocouples allow us to monitor the condition of the different parts of the gun and of the vaporizing assembly.

D. Sequence of operation and electrical power requirements

The gun is operated in consecutive steps. The filament is heated to produce an electron beam accelerated to the cathode which, in its turn, supplies a second electron beam to heat the hot plate. We find that there is a threshold in the current flowing to the hot plate above which the heating power is sufficient to maintain the cathode emission via heat radiation from the hot plate. When the current (cathode to hot plate) is over 1 A, one can safely operate the gun without the other supplies. Table 1 shows the general power requirements.

The power requirement is 2 to 3,5 kW (2.3 A and 1.2 kV are typicalworking parameters). In Fig. 4, we present temperature measurements of the hot plate and cathode showing the dependence on cathode-hot plate input power. We notice that the LaB_6 cathode temperature increases faster than the hot plate temperature. This

characteristic shows that we might have some process other than blackbody emission from the hot plate suppling heating power to the cathode. The cathode hot plage current is higher than one would expect under space charge limiting conditions. This may indicate the presence of metal ions in the cathode hot plate diode. We show in Fig. 5 the I-V characteristic of the gun which was determined at thermal equilibrium by reducing the incident power. This was the only way to work below 1 A emission. The tendancy of the gun to work at constant voltage, suggests that power regulation is best accomplished by current stabilization.

The power requirements for the vaporizing assembly are relatively small. The total power is 600 W for the two supplies. The use of current regulation leads to a constant vaporized barium flux. A layout of the combined system - source and power supplies - is shown in Fig. 6.

III. THE CHARACTERISTICS OF THE LINEAR MAGNETIZED PLASMA (LMP) DEVICE

The LMP device has been described in Ref. 5. The total length of the vacuum vessel is of the order of 9.2 m with an inner diameter of 0.40 m (Fig. 7). The vacuum vessel has a total of nine sections. At each end, two Tee sections allow coupling to the pumping stations. A total of 62 ports permit the access for diagnostics at 88 different axial and azimuthal positions. This allows us to insert optical diagnostics, probes and RF antennas, as well as anodes to change the length of the plasma. The vacuum vessel is made of stainless steel (AISI 316L) which insures a ferrite concentration less than 1% after the welding and machining.

The seven sections inserted inside the magnetic field coils are water cooled on the outer diameter as well as at the main flanges. A base pressure, with all diagnostics and plasma sources installed of around 1.10^{-7} torr is obtained. Ionization gauges installed in the plasma region are placed on an extension tube so that measurements are only slightly affected by the magnetic field.

The linear homogeneous magnetic field is created by 44 identical water cooled copper coils. An air cooled heat exchanger of 200 kW is used in a closed water circuit to maintain an input cooling water temperature below 60°C. Each coil is formed from two independent two-turn nine-layer pancakes which are sandwiched together. Each of the pancakes is individually water cooled.

A magnetic field of .3 Tesla is created by means of a current of 850 A. The current is regulated to compensate for long term drifts. This is accomplished by connecting a 40kW power supply in series with the 200kW main power supply. The current fluctuation at 300Hz is less than 0.01 percent because of the large time constant due to high coil inductance ($\sim 5.10^{-2}$H). The field homogeneity is 0.3% over a central length of 4.75 m and a diameter of 0.2 m. The plasma length may use the totality of the homogeneous B field. The thermal bi-metal security switches monitor the temperature of the water inlet and outlet of each pancake. A microprocessor control system periodically scans through these security interlocks in order to shut down the power supplies in the event of a fault or overheating. As a Q-machine, the LMP is currently the largest machine of this type, as of this writing.

IV. POWER SUPPLY CONTROL

The electrical block diagram of the LMP-Q device is shown in Fig. 8.

a) The current to the magnetic field is controlled by means of a microprocessor controller. The regulator has a PI (Proportional Integral) response in order to maintain the current within ± 1 A of nominal current settings. The measurement of the current is provided by means of a shunt with a .1% class of accuracy. The microprocessor controller with Motorola 6800 processor takes care of all the securities and safety interlocks and permits both power supplies (200 kW and 40 kW) to work together. All the convertors - A/D and D/A - have 12 bit resolution.

b) Each of the power supplies for the Q plasma source is controlled independently. Each contains its own PI regulator. The desired value for each particular current is preselected on the control panel, together with the stepping time, to allow us to rise to maximum values smoothly; the incident current value grows up linearly with the step increment until it reaches its maximum value. At each step, the control system maintains the currents constant. The growth rate (stepping time) of the current for each power supply could be adjusted individually.

The analog signals are led via a 16 channel multiplexer to a 12 bit A/D converter with maximum throughput 50kHz.

All the input signals are normalized to ± 5 V by means of operational amplifiers.

All important parameters regarding the status of the device arepermanently displayed - gun temperatures, gun currents and voltages, oven and heated pipe temperatures, chamber pressure, magnetic field as well as the status of the securities ... -.

A large TV video monitor is employed as a display. The screen has a hard copy facility at anytime, initiated manually.

V. PLASMA CHARACTERISTICS

In the LMP, the basic plasma parameters and behaviour are diagnosed by Langmuir probes and laser induced fluorescence. Ion saturation current Langmuir probes are used to measure density profiles along x and z. And also to monitor plasma density during operation.

In Fig. 9, we present density profile measurements. In Fig. 10 the floating potential and the electron saturation current radial profiles are shown. These two curves have a different shape than the ion density profile, showing stronger gradients, and defining the hot plate dimensions. Also, an edge step in the electron saturation current may indicate the tantalum can which has a stronger electron emission than rhenium.

Ion temperature is measured using laser induced fluorescence.[6] By scanning the frequency of a narrow band dye laser, one is able to observe fluorescence due to those ions which satisfy the Doppler resonance broadening condition:

$$-\frac{v_{\parallel}}{c} = \frac{\omega_L - \omega_0}{\omega_L}$$

where $v_{\parallel}$ is the component of ion velocity along the laser direction, ω_0 is the frequency of the ionic transition, ω_L is the laser frequency and c speed of light.

A partial grotrian diagram is shown on Fig. 11. This presents the two transitions which have been used starting from either the ground state or the metastable state of the barium ion.

A measured ion temperature profile is shown in Fig. 12. Also, by keeping the laser frequency fixed, we were able to detect the radial density profile by scanning the laser beam spatially on a horizontal cord. A density profile obtained by pumping the metastable state is presented in Fig. 13.

As it is well known, plasmas produced in a single ended Q device drift away from the source. Parallel velocity drift of the order of $1.2\ 10^5 cm \cdot s^{-1}$ has been measured from the corresponding line shifts. Also, a temperature difference between the parallel and perpendicular direction is evident from these measurements [Fig. 14]. A slow rotation of the plasma column has been measured by optical tagging.[7] The rotation velocity is of the order of $6.4\ 10^3 rad \cdot s^{-1}$. This plasma rotation was detected by means of an optical carriage which moves along Z and also accross X axis.

VI. CONCLUSIONS

We have developed a stable Q-machine with well determined parameters for long term times, of constant plasma density and temperature. The plasma characteristics and gun behaviour allow research in fundamental plasma physics, especially with the use of non perturbing powerful optical (LIF) diagnostics in the determination of many of the plasma parameters.

Aknowledgement

The authors express their gratitude to Drs F. Skiff, T. Good, M.Q. Tran and Prof. R.A. Stern for their support and many valuable discussions as well as for reading the manuscript. They also thank greatfully Dr. T. Good and F. Anderegg for the use of the fluorescent diagnostic results. The collaboration of Mr. J. Stramke, of the Laboratoire de Métallurgie Physique (EPFL) for brazing under vacuum the resistive coaxial wire to the oven and heated pipe, wasparticularly appreciated. They acknowledge deeply the work performed by the U.C. Irvine team and by the CRPP services (vacuum, mechanical, electrical and electronical workshops).

This work was supported by grants from the Fonds National Suisse de la Recherche Scientifique and by the U.S. National Science Fondation.

TABLE I

General power requirements for the CRPP gun

Filament heater power 62A; 6 volts (372 watts) (Joule-heating)

Filament — cathode power 0.5A; 1150 volts (575 watts) (electron bombardment).

Cathode — Hot plate heating 2.2A; 1200 volts (2.64 KW) (electron bombardment). The measured temperature of the hot plate (by optical pyrometer) for this power watts was ≈ 2130° K.

For the same power, the UCI gun shows a different hot plate temperature (2380° K). We do not understand this discrepancy, the plasma density is evaluated to be rather identical in both cases.

TABLE II

LMP-Q parameters

Barium	M = 138 a.m.u.	$M/m_e = 2.5 \times 10^5$
n_i	$10^8 < n_i < 10^{11}$ part/cm^3	
$T_i = T_e$	T ≈ 0.2 eV	
B field	.5 < B < 3kGauss	
Ion gyroradius	r_{gi} = 0.18cm for B=3KG and T_i=0.2eV	
Electron gyroradius	$r_{ge} = 3.67 \times 10^{-4}$cm for B=3KG	
Ion thermal velocity	$V_{thi} \approx 5.3 \times 10^4$ cm/s	
Ion drift velocity	$V_{di} \approx 1.2 \times 0^5$ cm/s	
Ion thermal energy	$T_i \simeq 0.2$ eV	
Ion drift energy	$E_{DI} \simeq 1.0$ eV	
Ion plasma freq	$f_{pi} \approx$ 565 KHz	for $n=10^9$cm^{-3}
Electron plasma freq	$f_{pe} \approx$ 284 MHz	for $n=10^9$cm^{-3}
Ion collision rate	ν_{ii} = 4.8KHz	for $n=10^9$cm^{-3}
Electron collison rate	ν_{ee} = 0.29MHz	for $n=10^9$cm^{-3}

References:

[1] N. Rynn and N. D'Angelo, Rev. Sci. Instrum. 31, 1326 (1960).
N. Rynn, Rev. Sci. Instrum. 35, No. 1, 40 (1964).

[2] R.W. Motley, "Q-machines", Academic press, 1975

[3] V. Laul, N. Rynn, and H. Böhmer, Rev. Sci. Instrum. 48, No. 11, 1499 (1977).

[4] P.J. Paris et al., to be published.

[5] M.Q. Tran, P. Kohler, P.J. Paris, and M.L. Sawley, CRPP Laboratory Report LRP205/82 (1982).

[6] D.N. Hill, S. Fornaca, and M.G. Wickham, Rev. Sci. Instrum. 54, 309 (1983).

[7] F. Anderegg, P.J. Paris, F. Skiff, T.N. Good, and M.Q. Tran, to be published in Rev. of Sci. Instrum.

Figure Captions

Fig. 1: a) Layout of the Q-source gun

b) Opened 3D view of the gun

Fig. 2: a) 3D presentation of the gun with barium oven, heated pipe (neck) and effuser

b) Detailed presentation of different interfaces of the vaporizing assembly

Fig. 3: Integration of the Q-source into the water-cooled jacket placed inside the vacuum vessel

Fig. 4: a) Hot plate and cathode temperature versus input power (cathode-hot plate). Measurements were performed at U.C. Irvine.
One remarks the difference of slop of both curves which implies other mechanisms of heating than black-body radiation.

b) The behavior of the CRPP gun is shown in parallel with UCI's gun. The S-B law (Stefan-Boltzmann) shows different behaviors of the two parallel slopes from the two guns (UCI and CRPP).

Fig. 5: Current-voltage behavior of CRPP's gun (cathode-hot plate values)

Figure Captions (cont'd)

Fig. 6: General layout of the barium Q-source with relative power supplies. T_1 to T_4 represent the thermocouples. The oven and the heated pipe (neck) are also powered by microprocessor-controlled supplies.

Fig. 7: General view of the experiment. Also shown is the B-field strength along the device.

Fig. 8: Electrical block diagram of the LMP device.

Fig. 9: Electron density profiles: a) radial
b) axial

Fig. 10: a) Radial ion saturation current and electron saturation current of a biased probe moving across the plasma. The electron saturation current shows sharp edges, related to small Larmor radius and to different emissions from the tantalum tube holding the tungsten hot plate.

b) Radial floating potential profile taken by a probe moving across the plasma.

Fig. 11: Grotrian diagram for Ba II: $5^2D_{1/2}$ and $5^2D_{3/2}$ are the metastable states (life time ~1s).

Fig. 12: Radial ion temperature taken by laser fluorescence technique.

Figure Captions (cont'd)

Fig. 13: Radial density profile: measurement performed by pumping the metastable state $5^2D_{3/2}$ and detecting the decay from the $6^2P_{3/2}$ state to the ground state (at 455.4 nm)

Fig. 14: Measurement of the velocity distribution functions: parallel and perpendicular to the axial magnetic field.

The measurements have been performed by a pulsed dye laser. The scannings along the wavelength show that $v_\perp > v_\parallel$ and allow measurements of the drift velocity along the B-field.

Photo 1 General view of the LMP experiment

Photo 2 } Q source installed on the positionning set-up jig
Photo 3 }

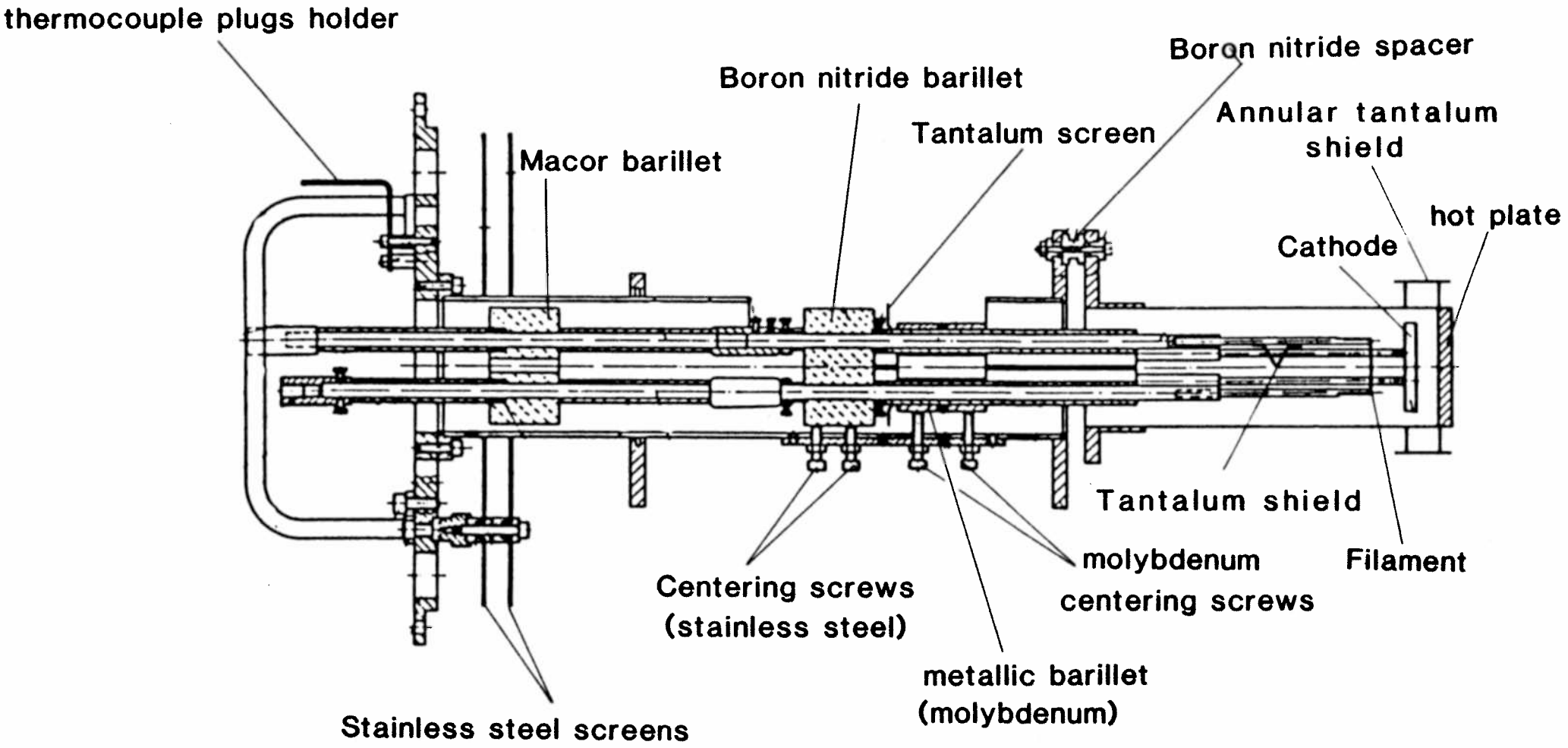

Q source gun

Fig.1a

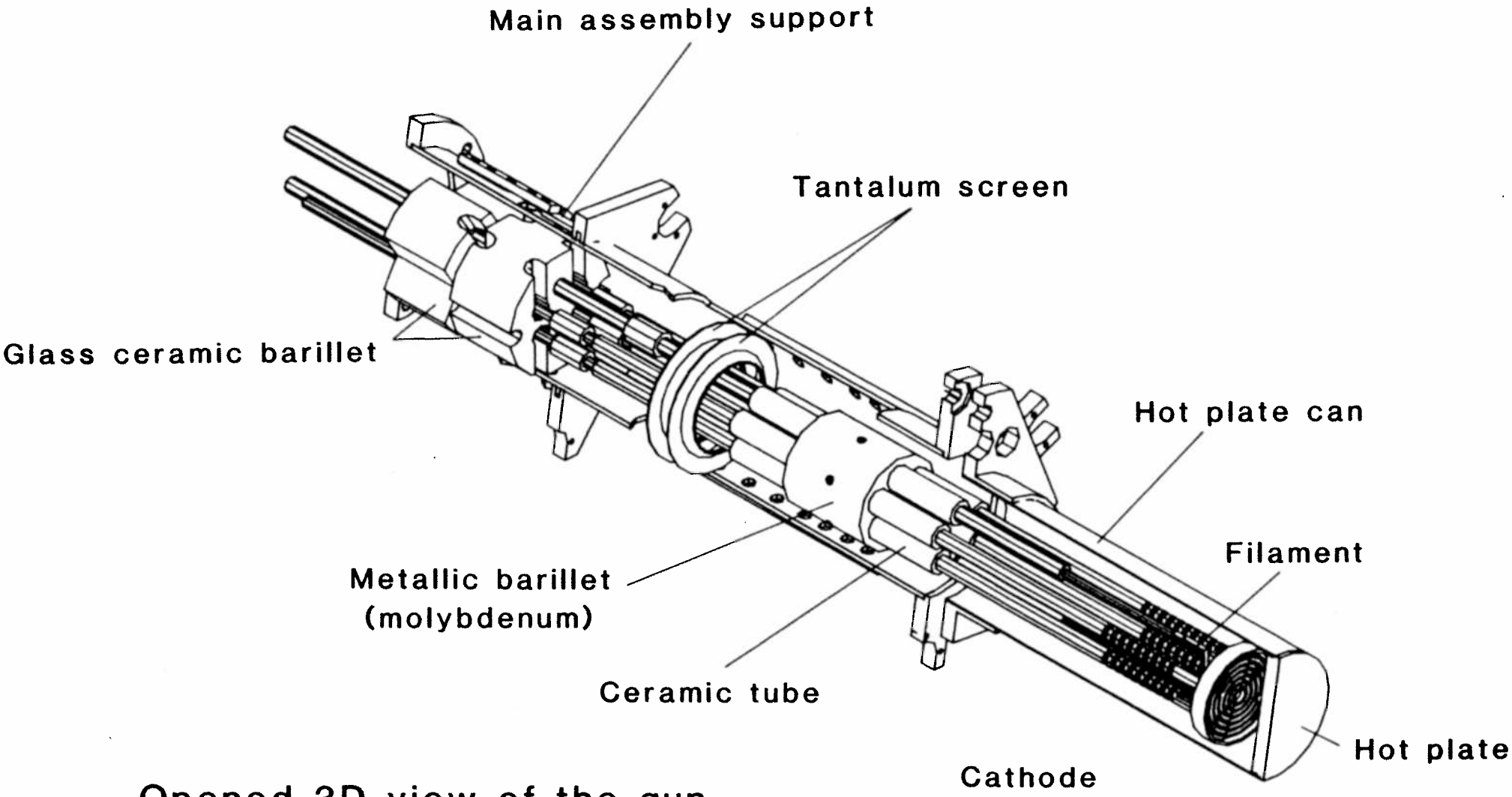

Opened 3D view of the gun

Fig.1b

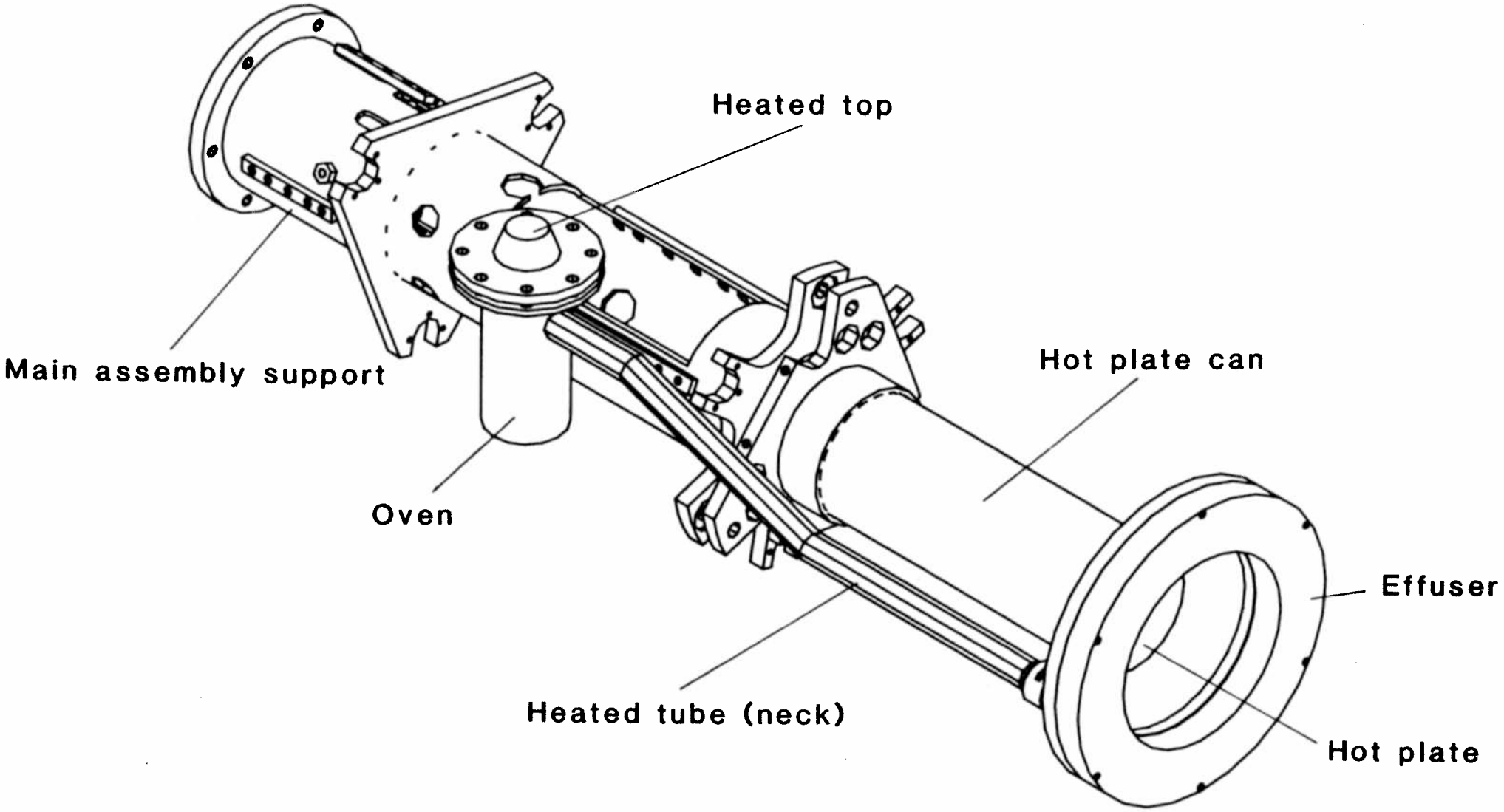

3D presentation of the gun with vaporizing barium subsystem

Fig.2a

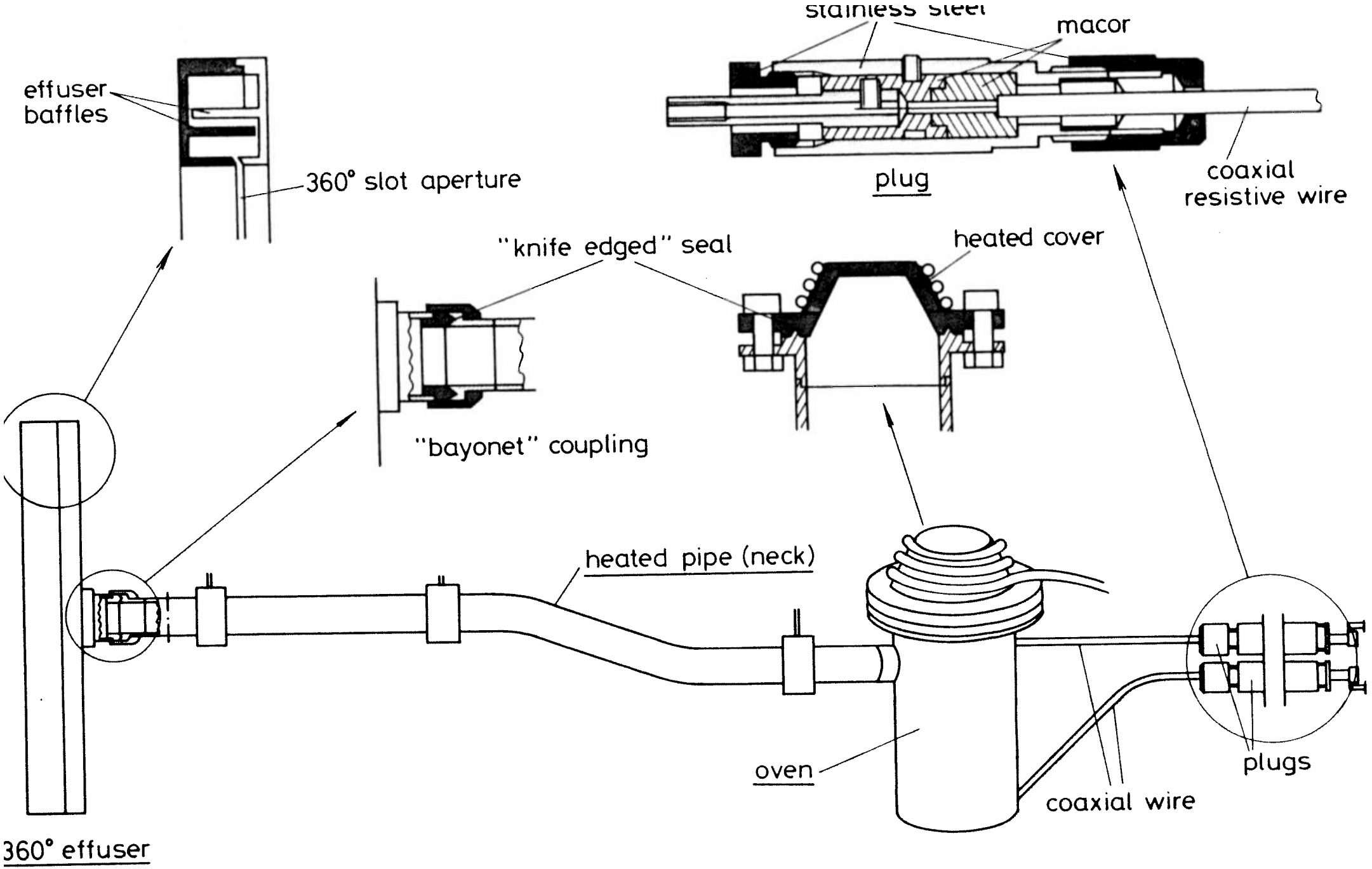

Barium Vaporizing Assembly
Fig.2b

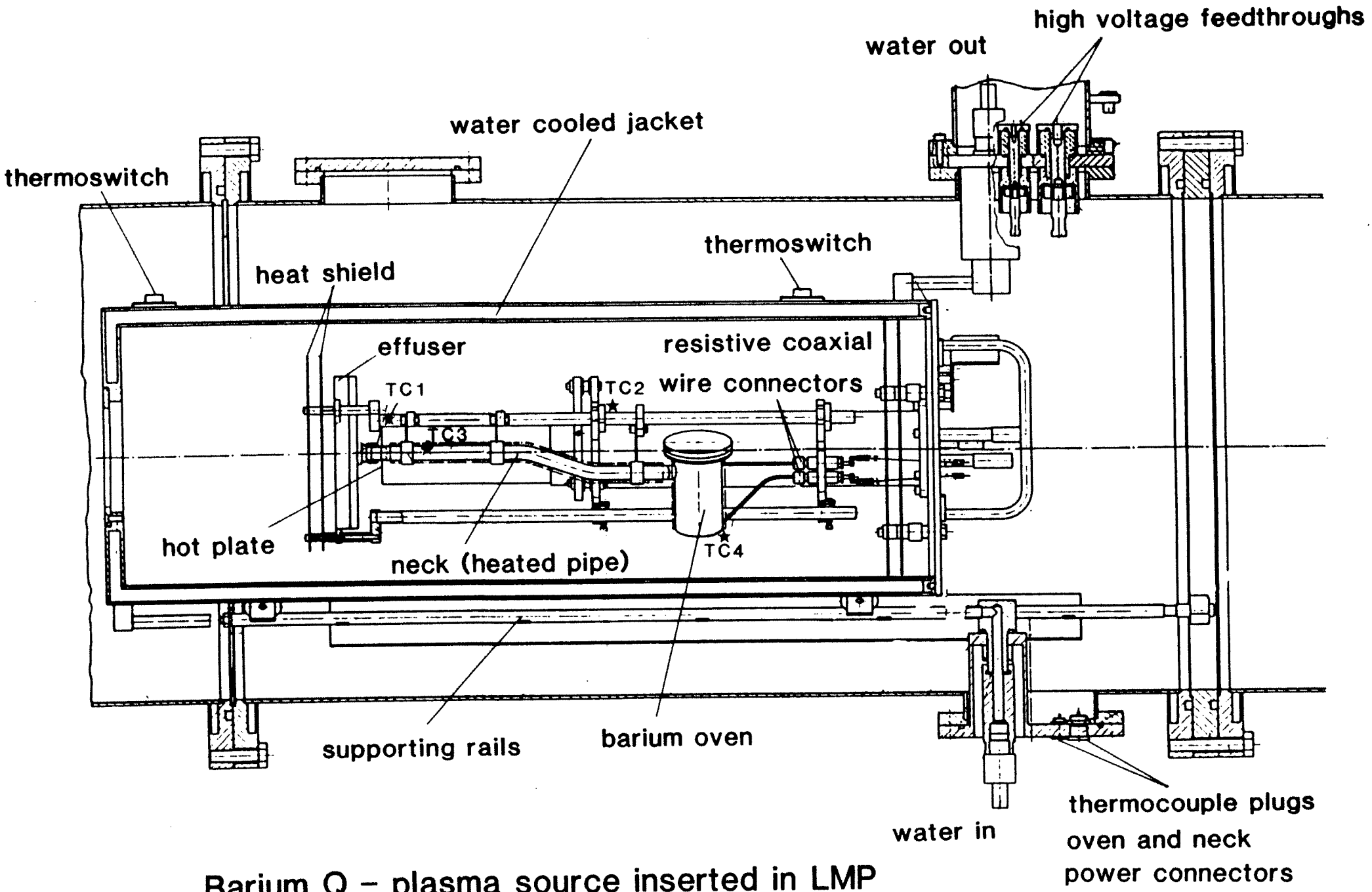

Barium Q,- plasma source inserted in LMP

Fig.3

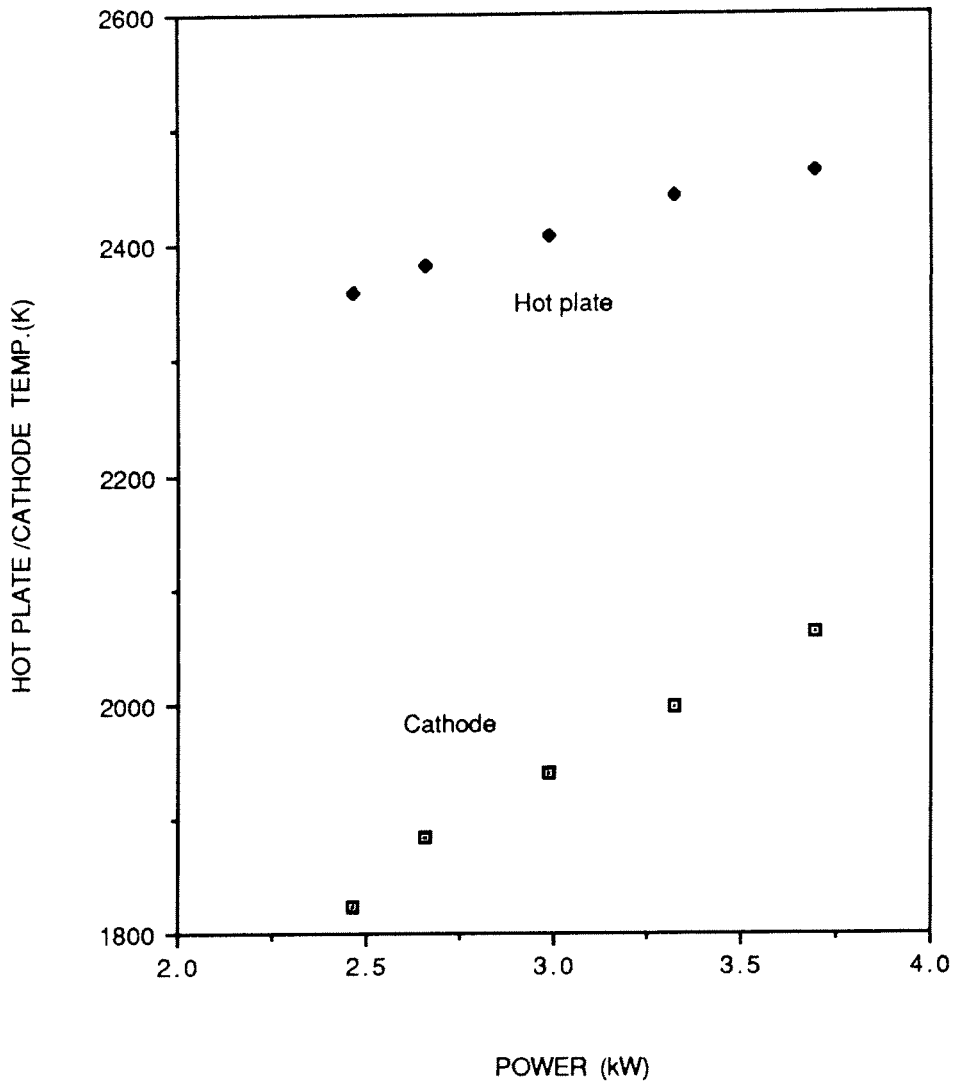
2600
2400
2200
2000
1800
HOT PLATE /CATHODE TEMP.(K)
Hot plate
Cathode
2.0
2.5
3.0
3.5
4.0
POWER (kW)

Fig.4a

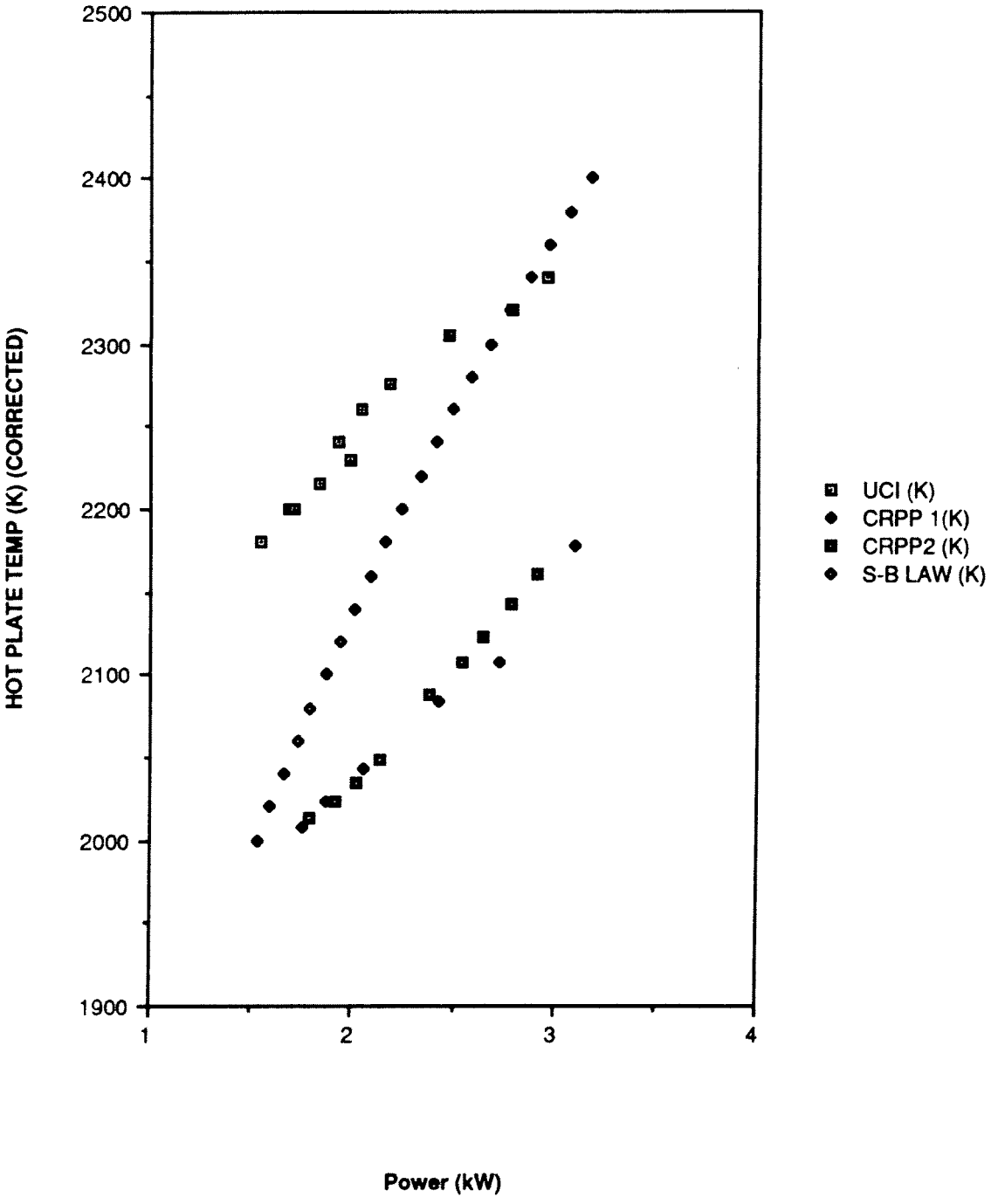
2500
2400
2300
2200
2100
2000
1900
1
2
3
4
HOT PLATE TEMP (K) (CORRECTED)
Power (kW)
UCI (K)
CRPP 1(K)
CRPP2 (K)
S-B LAW (K)

Fig.4b

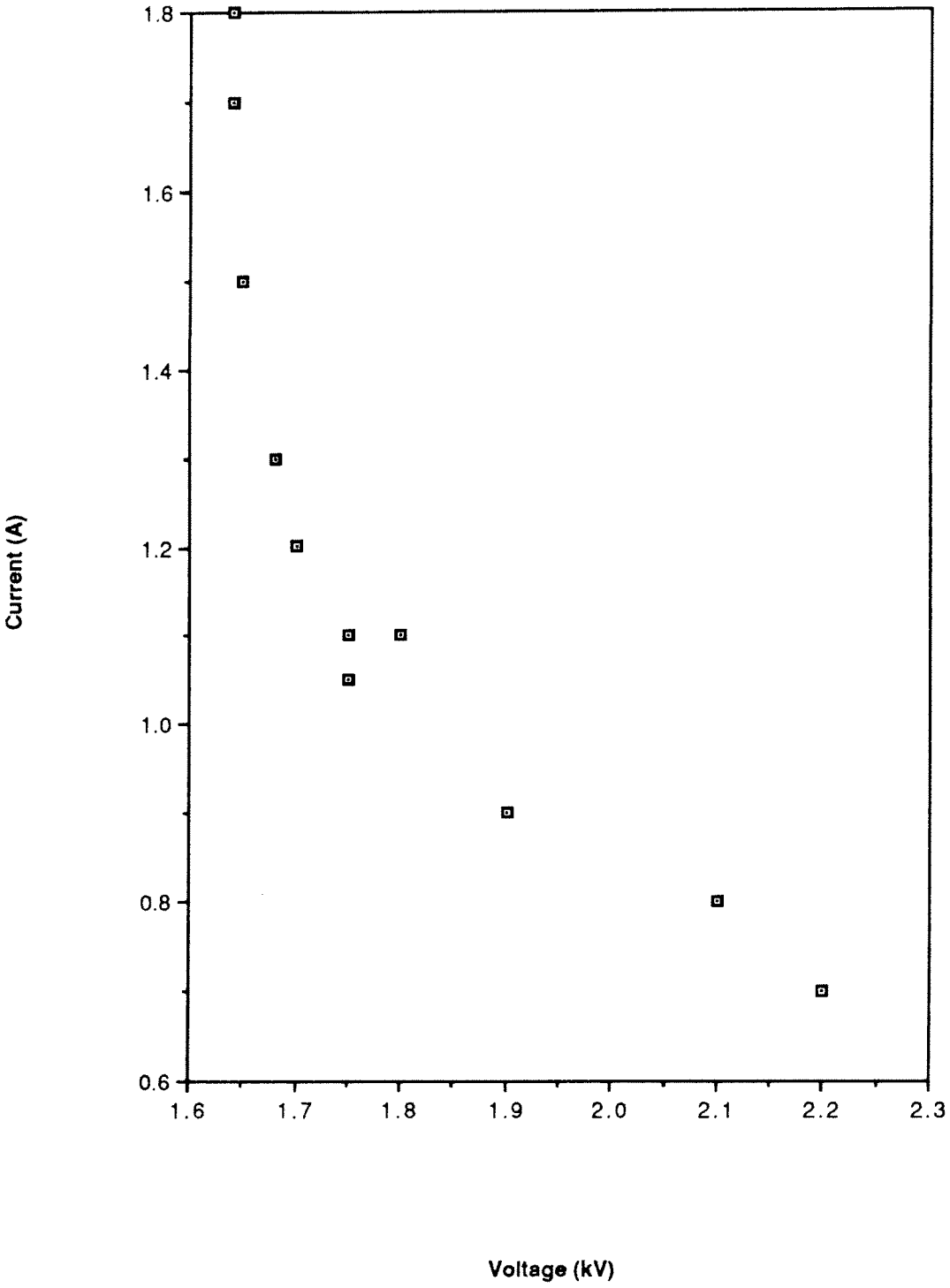

Fig.5

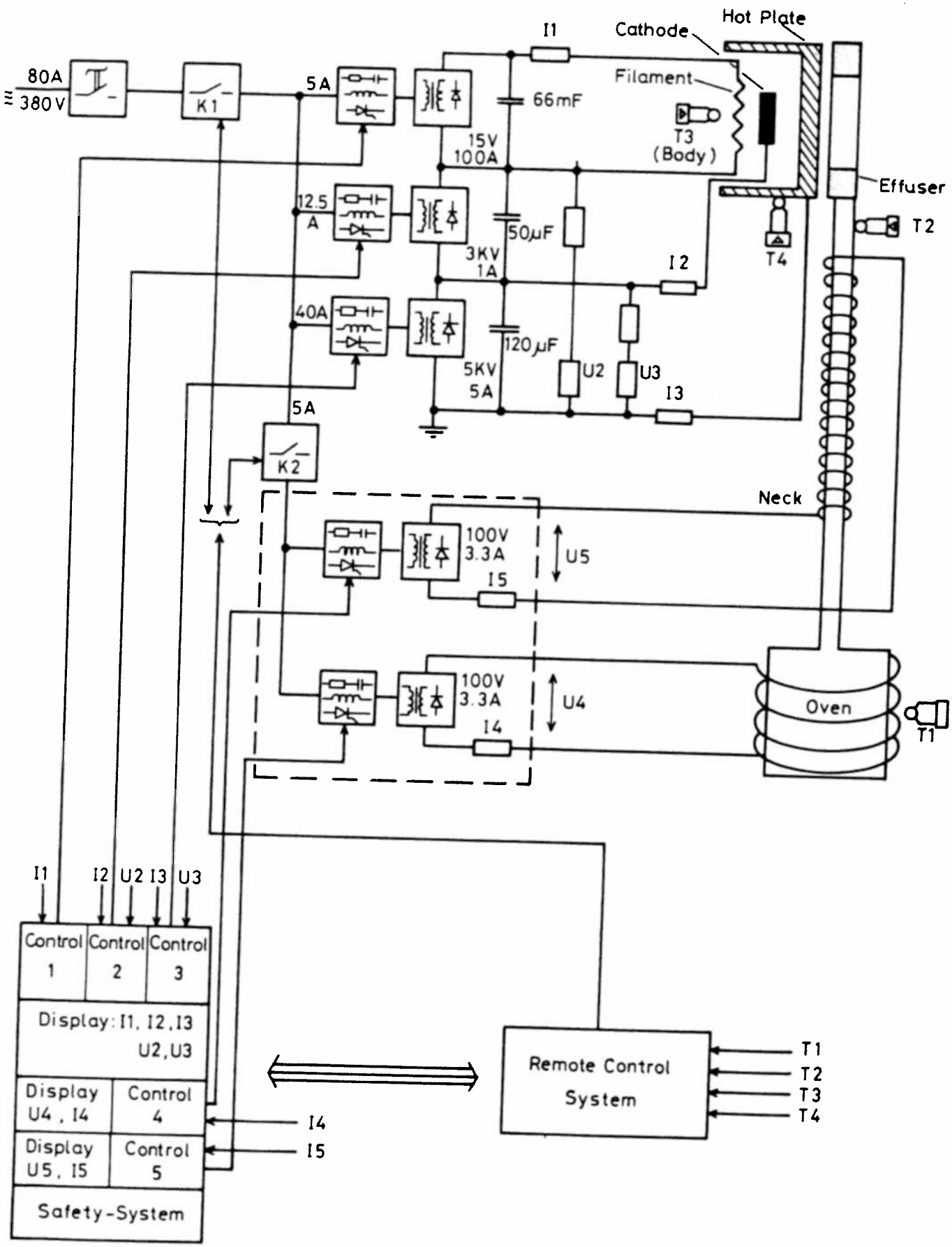
80A
≅ 380V
K1
5A
66mF
I1
Cathode
Hot Plate
Filament
T3
(Body)
15V
100A
Effuser
T2
T4
12.5
A
50µF
3KV
1A
I2
40A
120µF
5KV
5A
U2
U3
I3
5A
K2
Neck
100V
3.3A
U5
I5
100V
3.3A
U4
I4
Oven
T1
I1
I2
U2
I3
U3
Control 1
Control 2
Control 3
Display: I1, I2, I3
U2, U3
Display U4, I4
Control 4
Display U5, I5
Control 5
Safety-System
I4
I5
Remote Control System
T1
T2
T3
T4

Fig.6

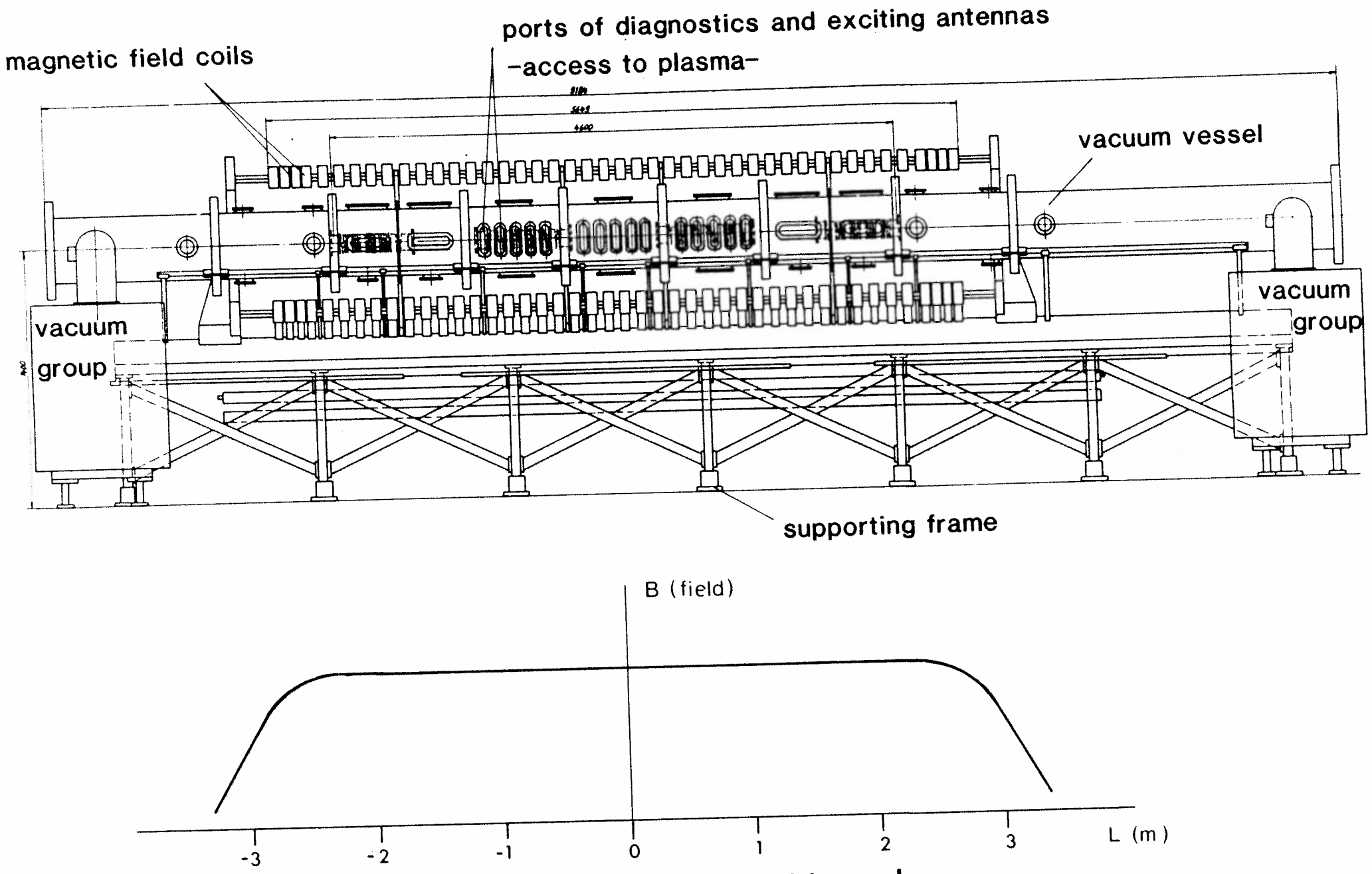

LMP – general view and B field graph –
Fig.7

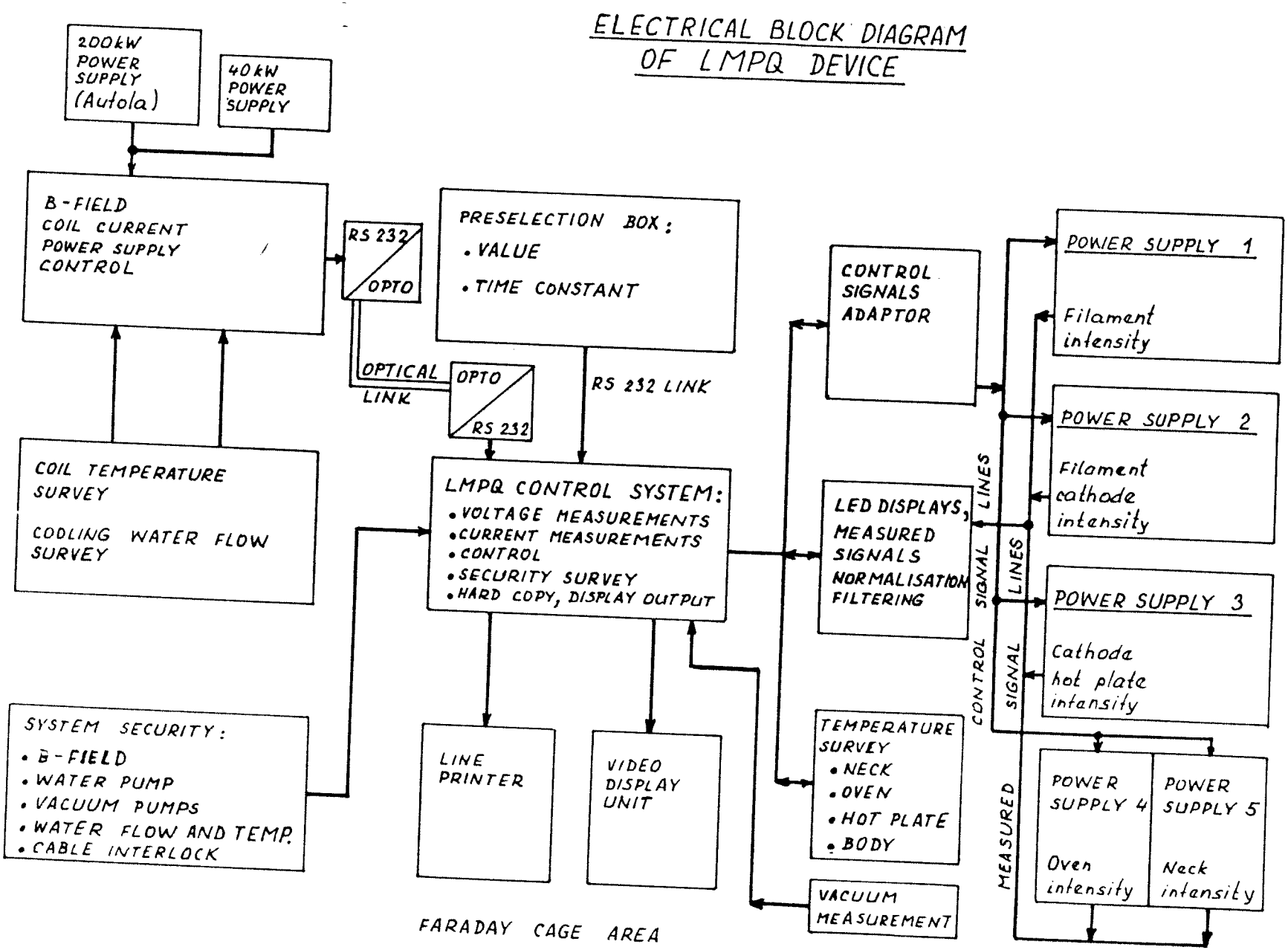
ELECTRICAL BLOCK DIAGRAM OF LMPQ DEVICE
200kW POWER SUPPLY (Autola)
40kW POWER SUPPLY
B-FIELD COIL CURRENT POWER SUPPLY CONTROL
RS 232 / OPTO
PRESELECTION BOX:
• VALUE
• TIME CONSTANT
OPTICAL LINK
OPTO / RS 232
RS 232 LINK
COIL TEMPERATURE SURVEY
CODLING WATER FLOW SURVEY
LMPQ CONTROL SYSTEM:
• VOLTAGE MEASUREMENTS
• CURRENT MEASUREMENTS
• CONTROL
• SECURITY SURVEY
• HARD COPY, DISPLAY OUTPUT
CONTROL SIGNALS ADAPTOR
LED DISPLAYS, MEASURED SIGNALS NORMALISATION FILTERING
CONTROL SIGNAL LINES
MEASURED SIGNAL LINES
POWER SUPPLY 1
Filament intensity
POWER SUPPLY 2
Filament cathode intensity
POWER SUPPLY 3
Cathode hot plate intensity
POWER SUPPLY 4
Oven intensity
POWER SUPPLY 5
Neck intensity
SYSTEM SECURITY:
• B-FIELD
• WATER PUMP
• VACUUM PUMPS
• WATER FLOW AND TEMP.
• CABLE INTERLOCK
LINE PRINTER
VIDEO DISPLAY UNIT
TEMPERATURE SURVEY
• NECK
• OVEN
• HOT PLATE
• BODY
VACUUM MEASUREMENT
FARADAY CAGE AREA

Fig.8

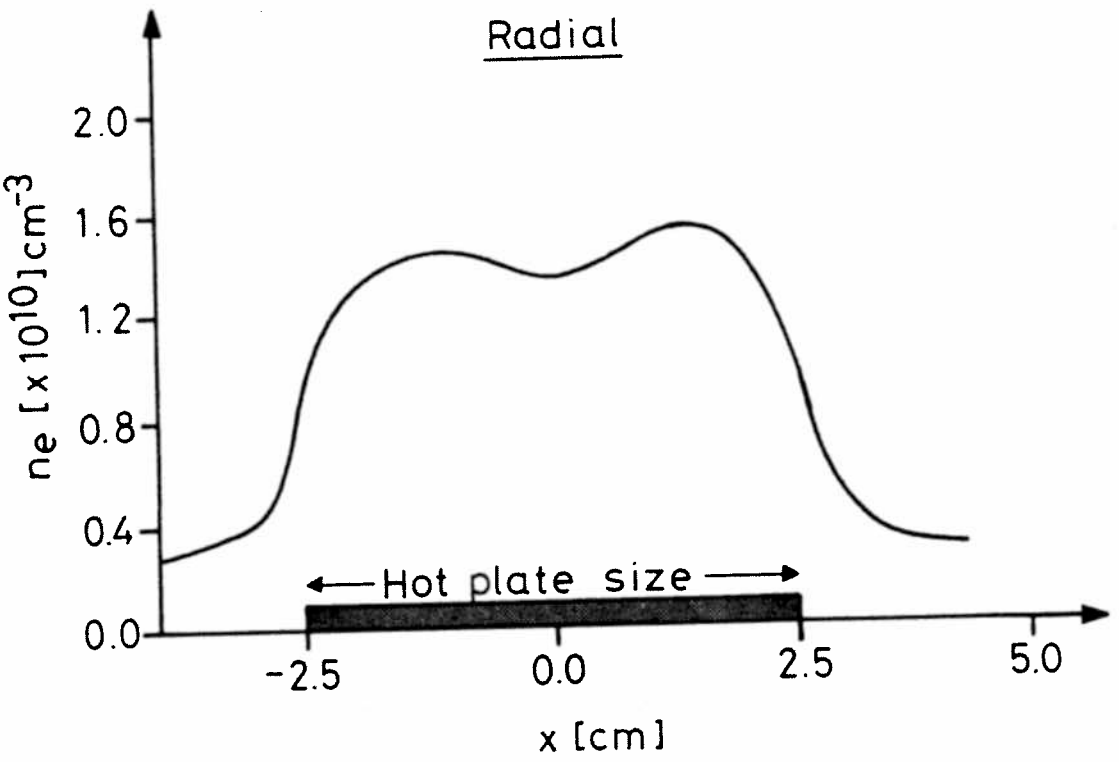

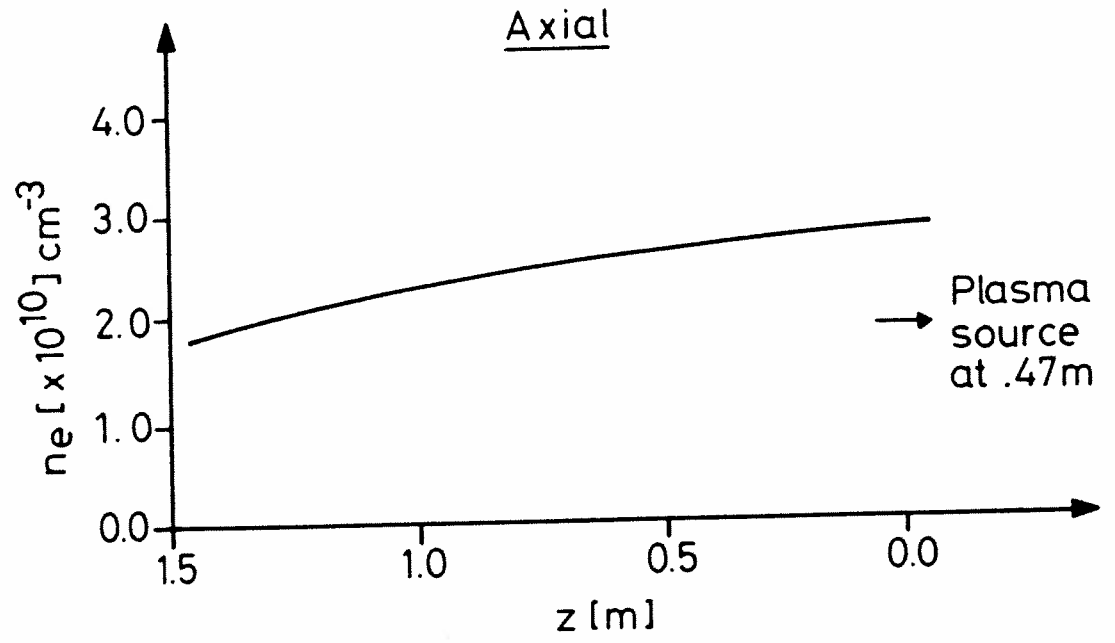

Density Profiles

Fig.9

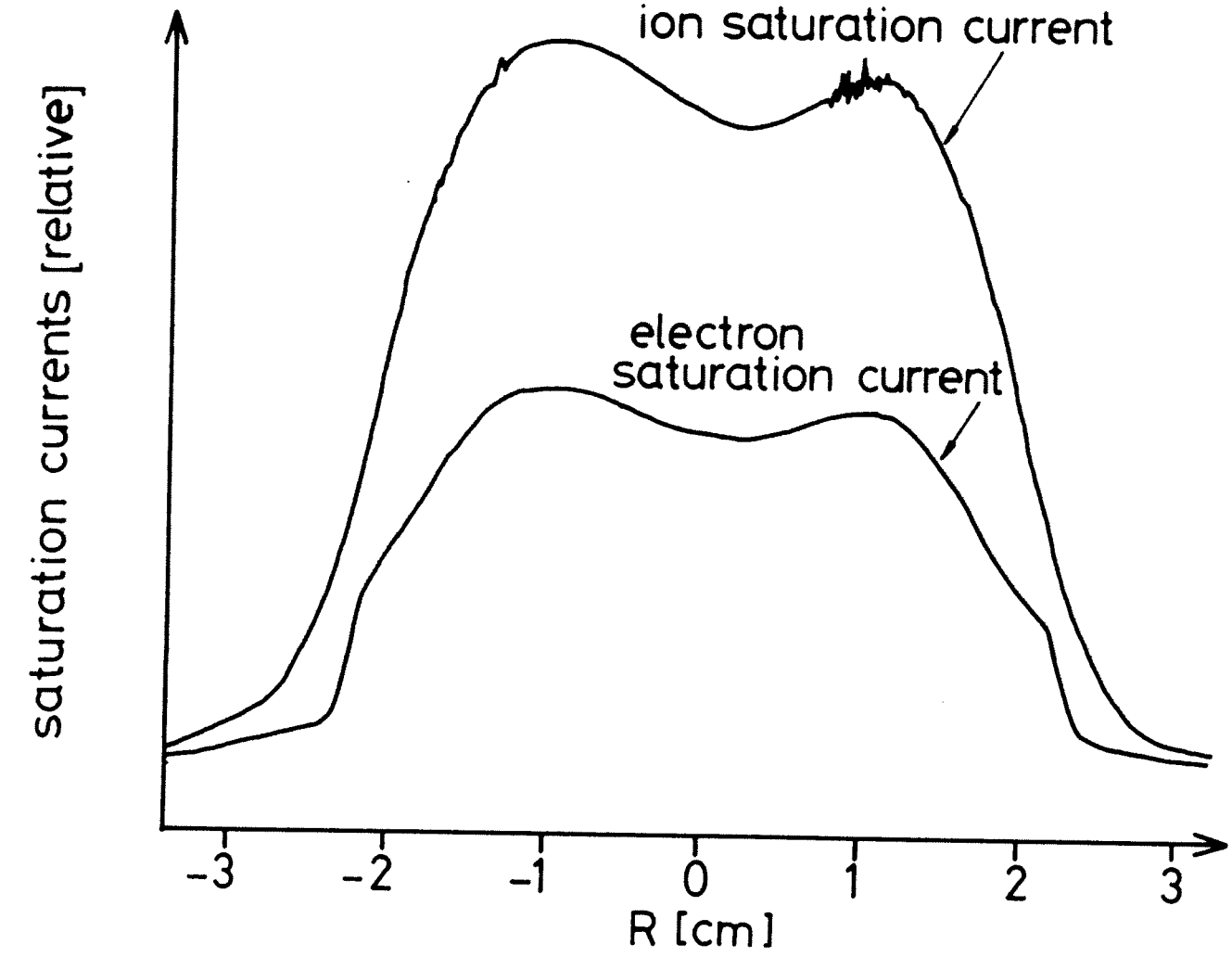

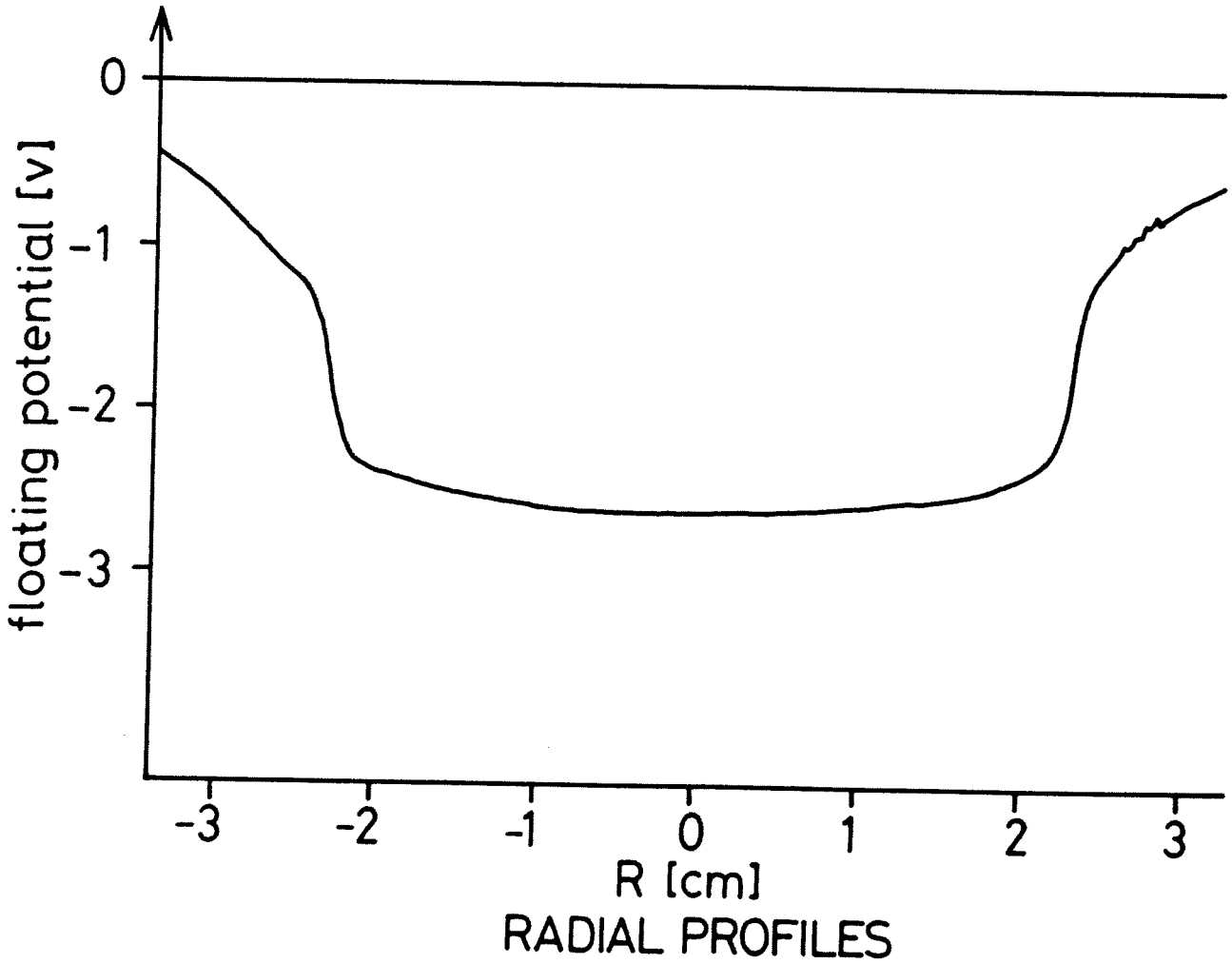

RADIAL PROFILES

Fig. 10

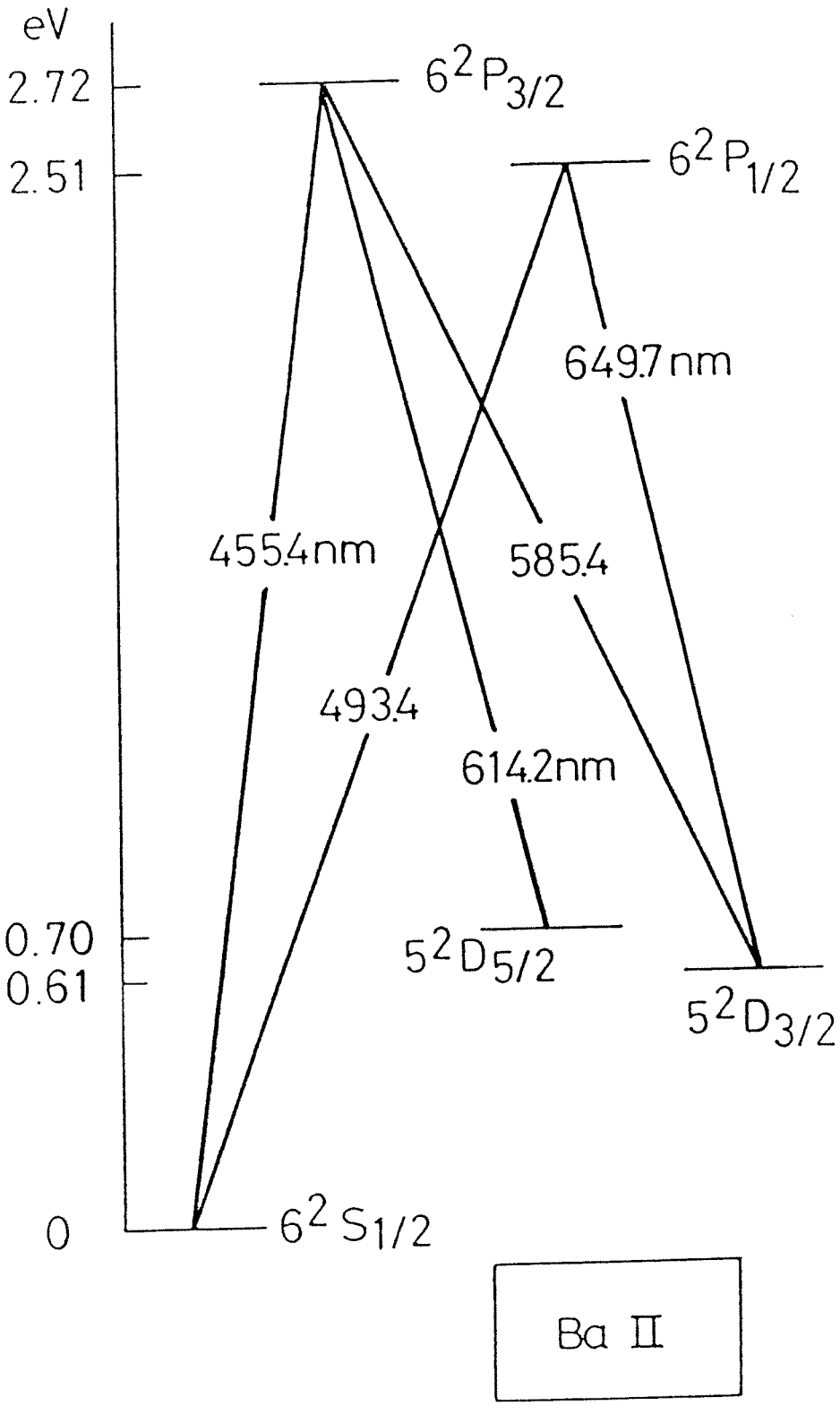
eV
2.72
2.51
0.70
0.61
0
$6^2P_{3/2}$
$6^2P_{1/2}$
$5^2D_{5/2}$
$5^2D_{3/2}$
$6^2S_{1/2}$
455.4nm
493.4
585.4
614.2nm
649.7nm
Ba II

Fig. 11

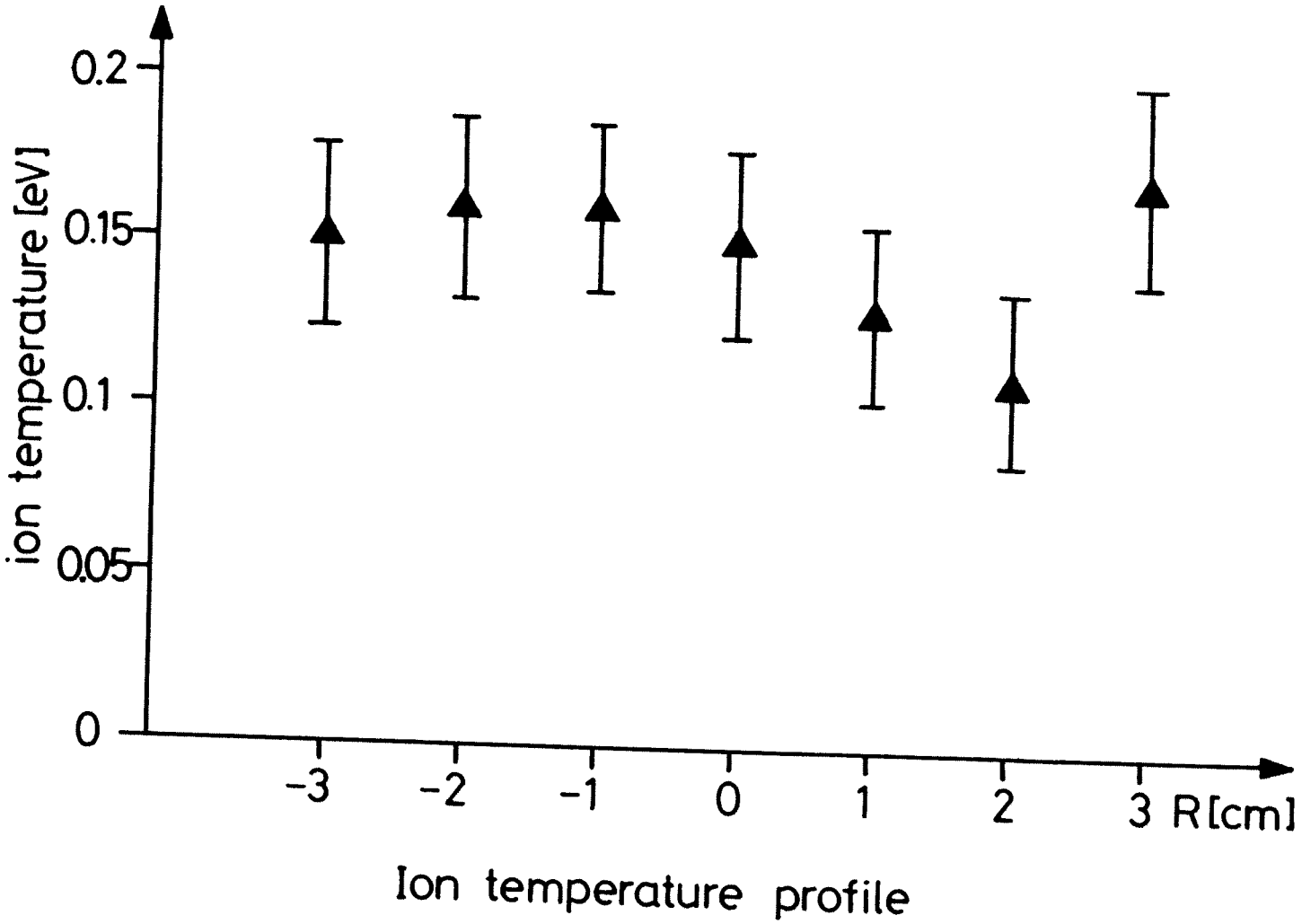
0.2
0.15
0.1
0.05
0
ion temperature [eV]
-3
-2
-1
0
1
2
3 R[cm]
Ion temperature profile

Fig. 12

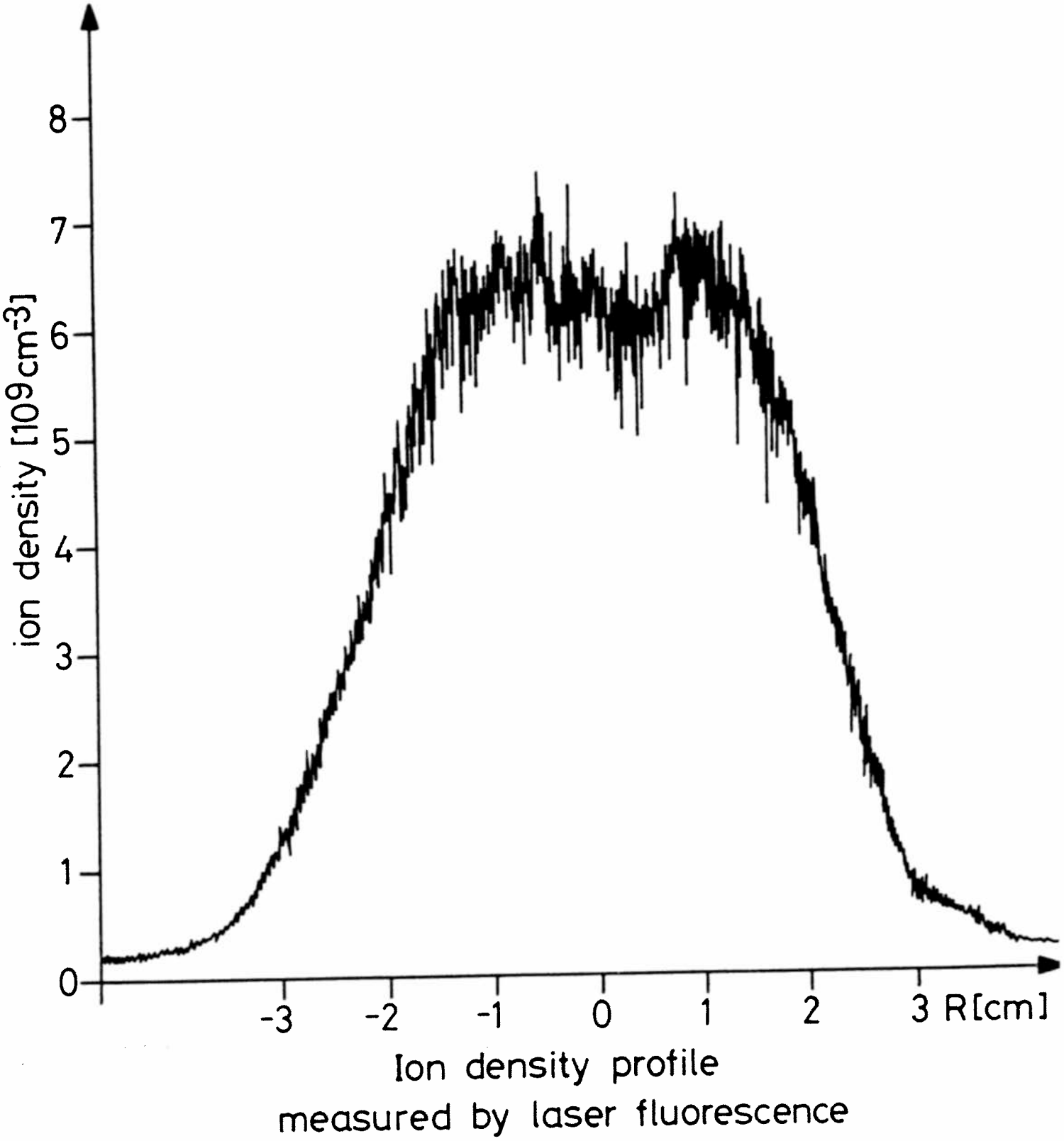

Ion density profile
measured by laser fluorescence

Fig. 13

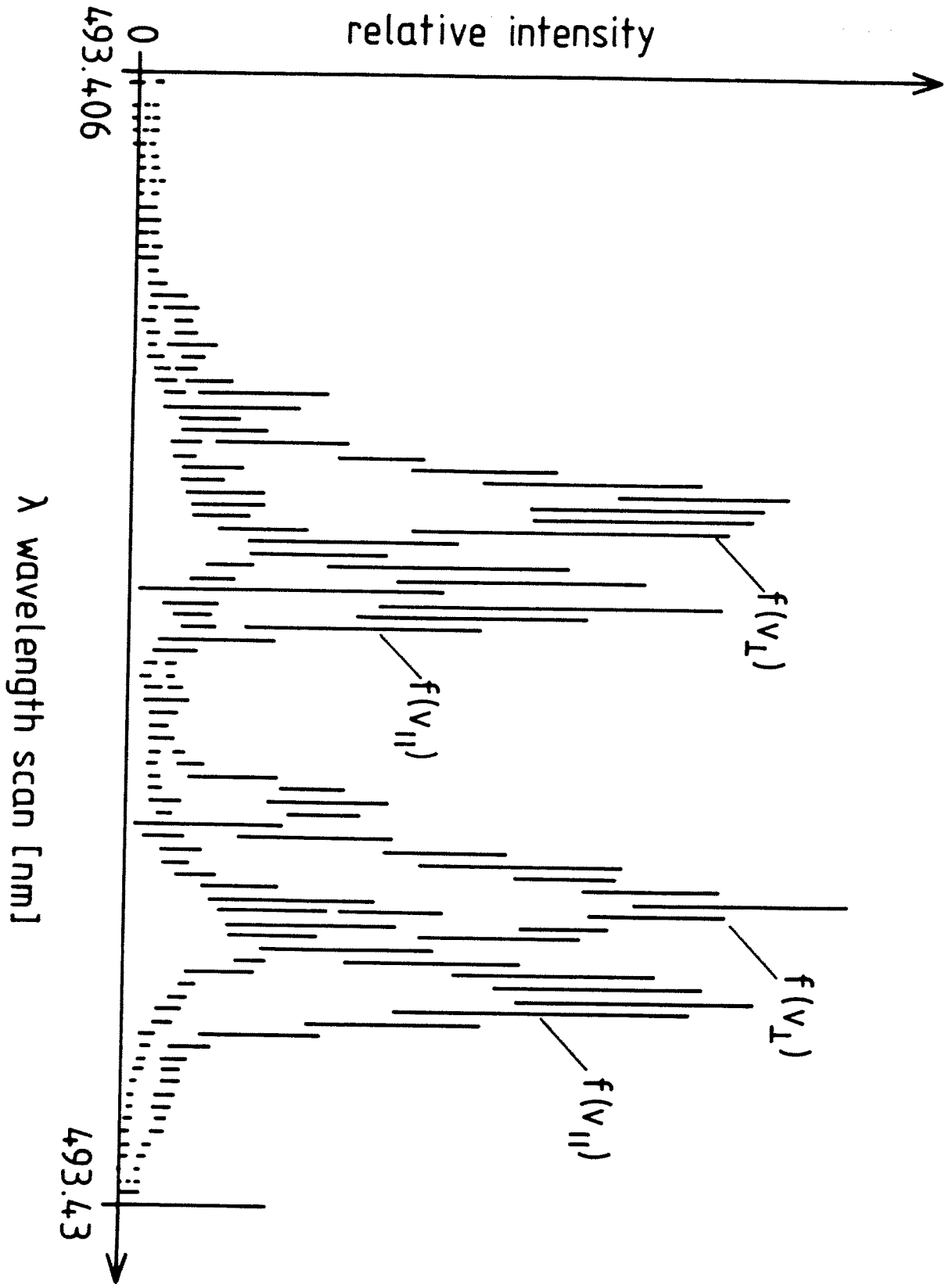
relative intensity
0
493.406
493.43
λ wavelength scan [nm]
f(v⊥)
f(v∥)
f(v⊥)
f(v∥)

Fig. 14

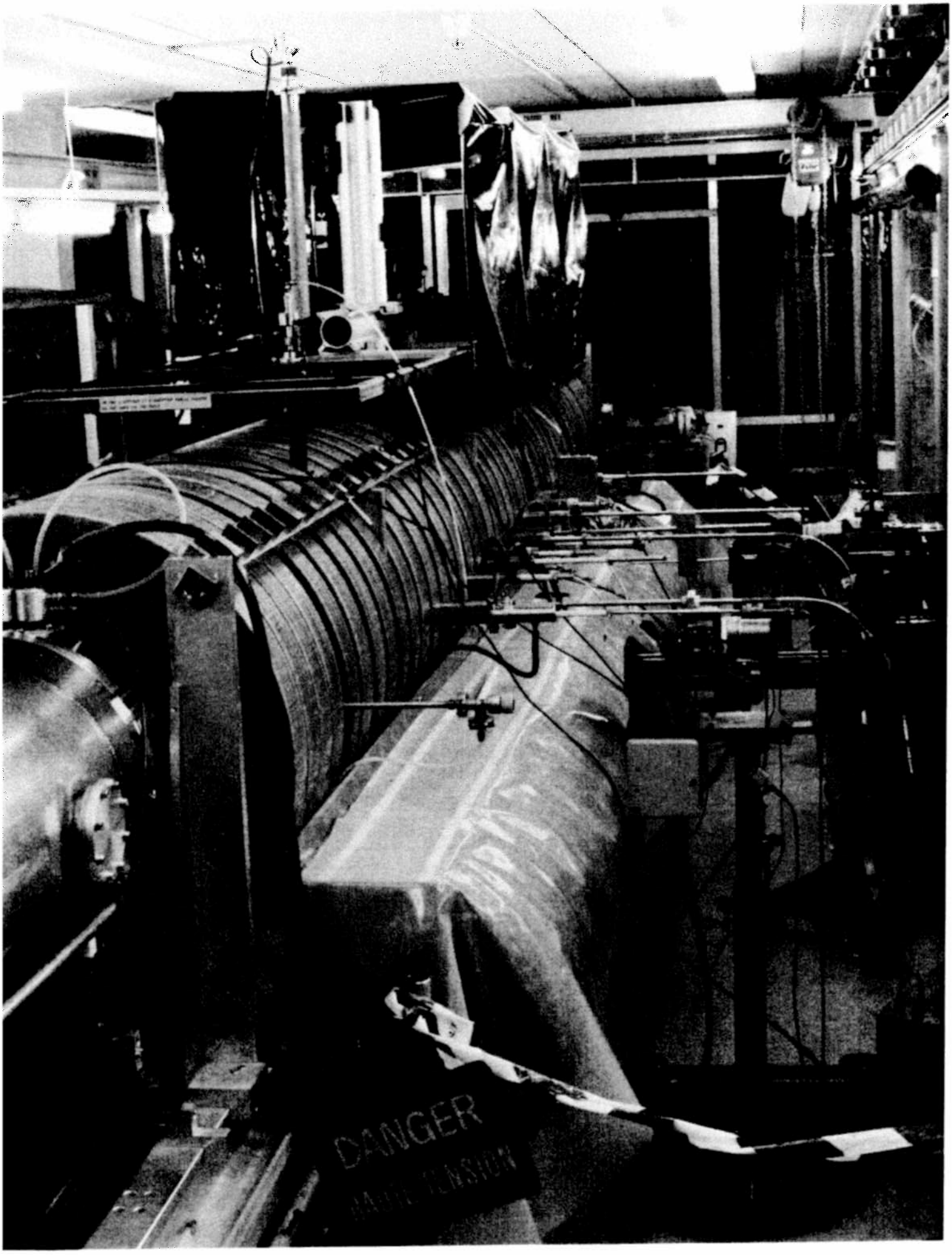

Photo 1

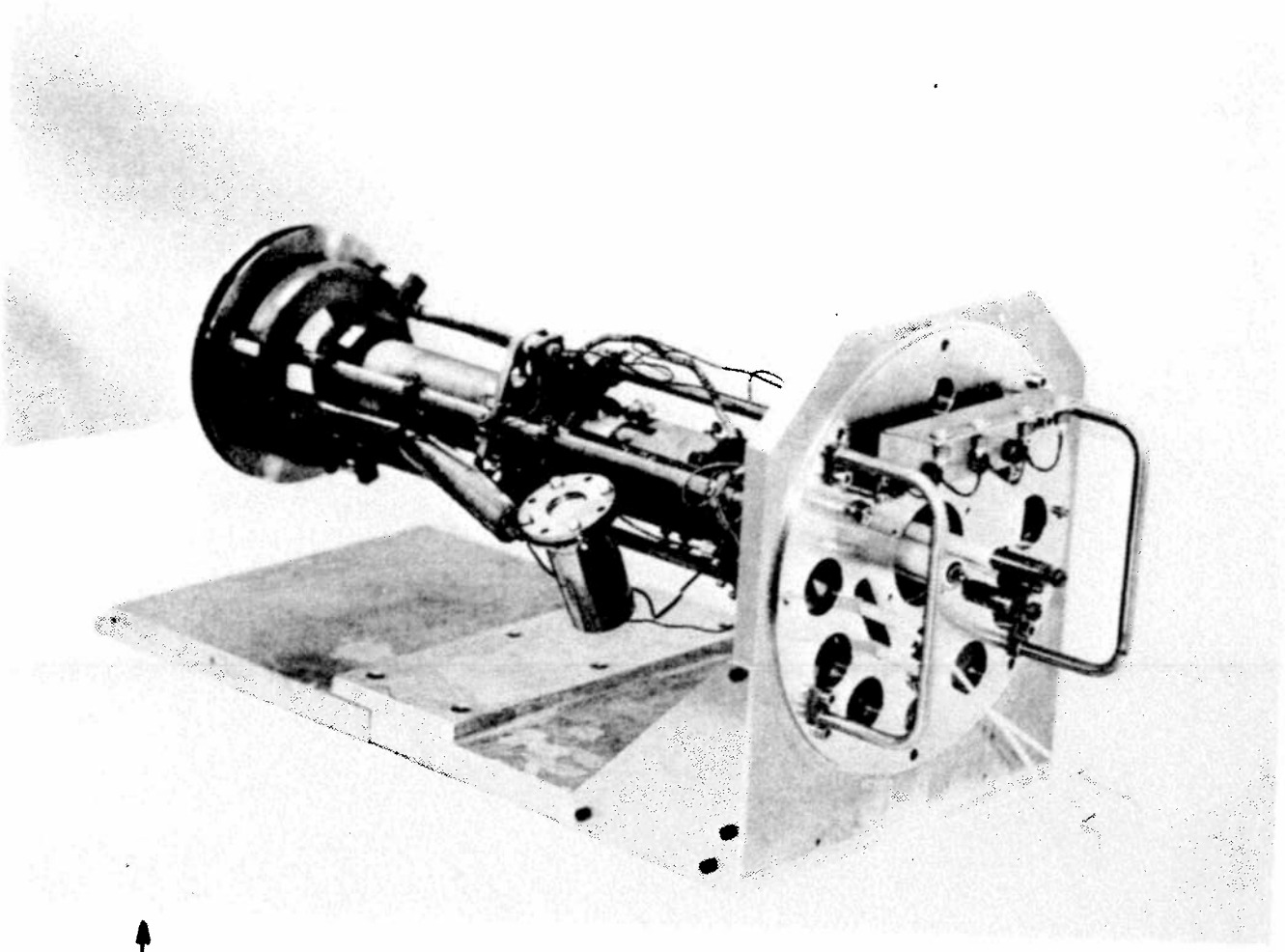

Photo 2

Photo 3